EXPERIMENTAL STUDY ON FLAME CHARACTERISTICS OF CRYOGENIC HYDROGEN JET FIRE

Xing Yu[1, 2], Yue Wu[1, 2], Yanqiu Zhao[1, 2] and Changjian Wang[1, 2]
[1] School of Civil Engineering, Hefei University of Technology, Hefei, Anhui 230009, PR China
[2] Anhui International Joint Research Center on Hydrogen Safety, Hefei, 230009, PR China

ABSTRACT

In this work, cryogenic hydrogen fires at fixed pressures and various initial temperatures were investigated experimentally. Flame length, width, heat fluxes and temperatures in down-stream regions were measured for the scenarios with 1.6-3 mm jet nozzle, 106 to 273 K, 2-5 bar_{abs}. The results show that the flame size is related to not only the jet nozzle diameter but also the release pressure and initial temperature. The correlations of normalized flame length and width are proposed with the stagnation pressure and the ratio of ambient and stagnation temperatures. Under constant pressure, the flame size, total radiative power and radiation fraction increase with the decrease of temperature, due to lower choked flow velocity and higher density of cryogenic hydrogen. The correlation of radiation fraction proposed by Molina *et al*. at room temperature is not suitable to predict the cryogenic hydrogen jet fires. Based on piecewise polynomial law, a new correlation of the radiative fraction is presented as a function of global flame residence time.

1 INTRODUCTION

Compared with high-pressure gaseous storage method, cryogenic storage technology can greatly improve the density of hydrogen which can bring great economic advantages in the future hydrogen economy [1]. The storage requirement of cryogenic hydrogen is different from traditional industrial flammable cryogens that are not space-constrained and can accommodate large safety separation distances [2]. To develop specifications and standards for the management of cryogenic hydrogen storage and transportation, a thorough understanding of the characteristics of accidental release and dispersion, along with flame characteristics over a range of realistic scenarios and environmental conditions, is critical necessary [3].

For hydrogen diffusion and jet flame characteristics at room temperature, a large number of scholars have carried out experiments and simulations. Ruggles *et al*. [4] used high-speed Schlieren photography to image the jet exit shock structure, and measured the instantaneous hydrogen concentration downstream of the Mach disk by quantitative Planar Laser Rayleigh Scatter imaging. Li *et al*. [5] investigated the effect of aspect ratio of rectangular slot nozzles on the decay rate of hydrogen concentration along the jet centreline. In order to obtain the concentration and velocity decay of high-pressure, under-expanded jet, Birch *et al*. [6]–[9] proposed the "pseudo-source" approach, which can extend the correlations established for subsonic flow to supersonic flow. The researches about hydrogen jet fire mainly focused on critical parameters that govern the deterministic separation distance (or the hazard distance), such as flame length, width and radiant heat flux. Proust *et al*. [10] carried out hydrogen jet fire experiments with pressure up to 90 MPa and obtained an original set of data about flame characteristics. Schefer *et al*. [9] adopted the dimensionless Froude number to analyse a large number of experimental data about visible flame lengths and verified that lower-pressure engineering correlations can be extended to releases up to 413 bar (6000 psi) via "pseudo-source" approach. Mogi *et al*. [11] gave up the dimensionless Froude number to characterize the visual flame length, and directly used hydrogen pressure and nozzle diameter to characterize the flame length, and established the correlation. Molina *et al*. [12] proposed the flame residence time τ_G to analyze flame radiation fraction. The radiative fraction for a momentum dominated flame was found to be proportional to $\log_{10}(\tau_G)$. Besides, a large number of CFD simulations on hydrogen dispersion [13]–[19] and jet fires [20]–[23] have also been carried out. The previous researches on hydrogen leakage and combustion at room temperature provide a large amount of comparative data for

the research of cryogenic hydrogen. Unlike room temperature, extreme cold temperatures can condense or even freeze ambient air during spills, which can result in unique hazards that likewise need to be understood.

Some scholars have already performed related researches about the diffusion and combustion of cryogenic hydrogen. Giannissi *et al*. [24] simulated the release process of cryogenic hydrogen and studied the effect of humidity in the atmosphere on the vapour dispersion. The computational results showed that humidity has a great influence on the buoyancy of cryogenic hydrogen cloud, which is different from the hydrogen leakage at room temperature. Friedrich *et al*. [25] performed release and combustion experiments for cryogenic hydrogen jets with temperatures ranging from 34 to 65 K, pressures from 7 to 35 bar and nozzle diameter 0.5 and 1 mm. The measured overpressures and sound levels showed no hazards to exposed persons during ignition. Panda *et al*. [26] investigated cryogenic under-expanded hydrogen jet fires over a range of temperature (37-295 K), pressure (2-6 bar_{abs}) and nozzle release diameters (0.75-1.25 mm). The experiment results presented that the mean mole fraction of hydrogen at ignition is approximately 0.14 with negligible dependence on temperature and the visible flame length preserved the linear dependence on the square root of jet Reynolds number for cryogenic hydrogen jet fires. However, the correlation is not very consistent with some previous data [11] at room temperature. The radiant heat flux increases as hydrogen temperature decreases. Kobayashi *et al*. [27] carried out 49 sets of high-pressure cryogenic hydrogen ignition experiments. The supplied hydrogen has a maximum range discharge pressure of 80 MPa and a temperature adjustment range of 50-300 K. Same with Panda *et al*. [26], Kobayashi *et al*. also found that the flame length increases with the decrease of temperature, with an increase rate over 30%.

The goal of this work is to shed light on the scientific understanding of the combustion characteristics of cryogenic hydrogen jet fire. This paper is an extension of cryogenic hydrogen jet fire in previous studies with small nozzle diameters (≤ 1.25 mm). The jet nozzle diameters range from 1.6 mm to 3 mm. The experimental system was designed for a controlled release at fixed pressure and continuously decreasing temperatures, to study the thermo-physical properties of cryogenic hydrogen jet fires. In the present study, low temperature (as low as 106 K) hydrogen released formed under-expanded jet fire after ignition. The temperatures on the centreline of the jet nozzle were measured by 11 sets of K-type thermocouples for CFD validation. In future work, the combustion properties will be characterized using high temperature C-type thermocouple array, capable of global temperature field measurement. The radiative heat fluxes in the direction perpendicular to the release centreline were measured using radiometers. We developed correlations between the flow parameters and the flame characteristics, such as flame length, width and radiant heat flux from cryogenic hydrogen jet fires.

2 EXPERIMENTAL SYSTEM

In previous experiments of hydrogen jet fire, the mass flow rates and temperatures in the nozzles are usually used as key parameters for cryogenic hydrogen jet fires [25]–[27], while stagnation pressures and temperatures in the reservoirs are used in the hydrogen jet experiments at room temperature [9]–[11], [28]. The possible reason for this difference is that the pressure and temperature are easy to be measured and controlled at room temperature, however, under cryogenic conditions, the pressure of hydrogen deviates from the stagnation pressure after cooling process. Different experimental apparatuses and key parameters lead to different correlation forms at room temperature and cold temperatures. To unify the correlations at various temperatures, a stagnation chamber with 16 cm in diameter and 29 cm in length was installed in front of the jet nozzle to monitor the stagnation pressure and temperature of cryogenic hydrogen, similar to the experiments at room temperature. The stagnation chamber was located just prior to the jet nozzle to maintain a low flow Mach number (less than $1 \times 10{-}3$) [9]. At this Mach number, the measured pressures and temperatures in the stagnation chamber were in excellent agreement with the true stagnation conditions. The sketch of the cryogenic hydrogen release experimental system is shown in Figure 1. The opening of the pressure reducing valve of hydrogen storage cylinders was adjusted automatically to maintain a stable pressure in the stagnation chamber by increasing or decreasing hydrogen supply. In experiment, gaseous hydrogen flowed into a coiled stainless-steel tubing which was dipped inside a bath of liquid nitrogen. The

hydrogen could be cooled to about 80 K and then delivered to the stagnation chamber. A comparison of the stagnation temperature profiles for releases through 2 mm nozzle at different pressures is shown in Figure 2. The cooling rate in the stagnation chamber is positively related to the stagnation pressure. The cooling process from room temperature to 110 K takes 300 s under the pressure 5 bar_{abs}, while 400 s for 4 bar_{abs}. Both the pressure and temperature histories in stagnation chamber were recorded for the duration of each case. The pressure was measured with an intelligent diffusion-silicon pressure transmitter, while the temperature was measured using a thermal resistance. Both voltage outputs were digitized at a 60Hz rate and stored on a Rigol digitized storage scope for post-processing.

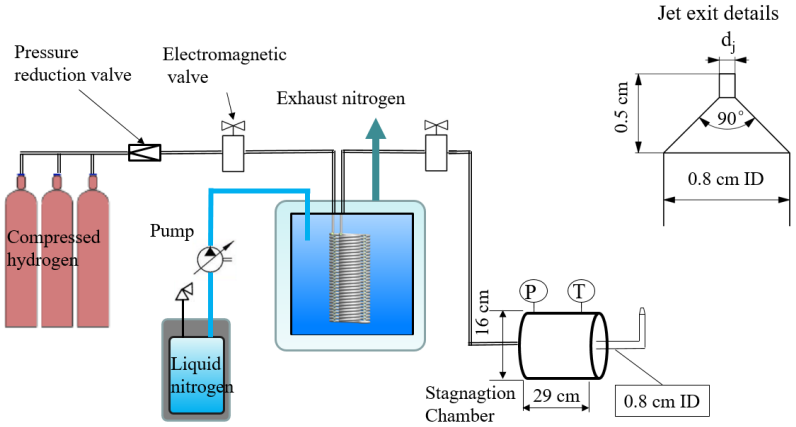

Figure 1. Schematic of the experimental system of cryogenic hydrogen jet fire.

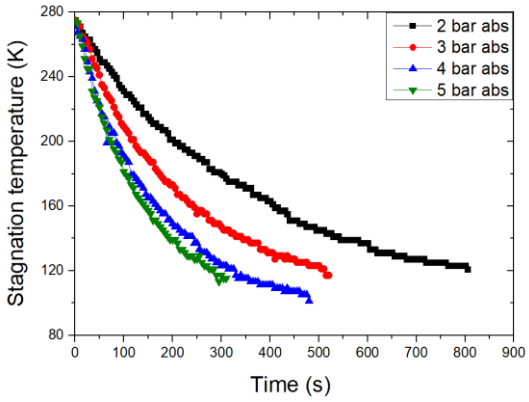

Figure 2. Temperature profiles in the stagnation chamber for cryogenic hydrogen releases through 2 mm nozzle.

The experimental operating conditions for the cryogenic under-expanded hydrogen release are summarized in Table 1. The pressure range was 2-5 bar, the temperatures varied from 106 to 273 K, and the jet nozzle diameters were switched between 1.6, 2 and 3 mm. The flow parameters at the jet nozzle were calculated assuming isentropic expansion from stagnation condition to sonic choked condition, using a real gas equation of state [9].

Table 1. Operating conditions of cryogenic hydrogen jet fire

Experimental parameters	Range
Pressure (bar_{abs})	2~5
Temperature (K)	106~273
Diameter (mm)	1.6, 2, 3

The flame length and radiant heat flux are critical parameters that govern the deterministic separation distance to prevent harm during an accident scenario [29]. In the present study, digital video images of the cryogenic hydrogen flames were obtained to characterize the flame shape, flame length and width. The flame images were recorded using Canon video camera and stored at a standard 50 fps video frame rate. Multiple flame images were extracted and averaged at selected times to provide quantitative data on the relevant flame length and width. The radiant heat fluxes were measured using 4 sets of Captec radiometers and the voltage outputs were collected by Hongge I-7018 module. Radiometers were placed at a radial distance, R, of 25 cm away from the jet centerline and at axial increments, Z, of 20 cm along the flame length as shown in Figure 3. Besides, the flame temperatures were measured using 16 sets of K-type thermocouples for future CFD validations. The thermocouples were placed 50 cm away from the jet nozzle at axial increments of 10 cm.

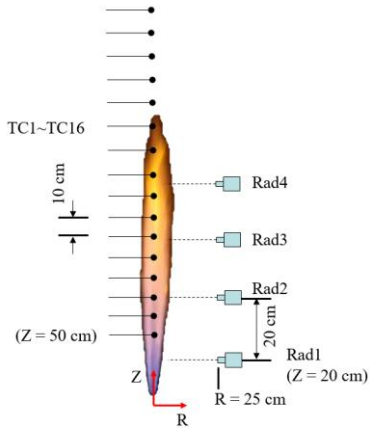

Figure 3. Schematic of the location of thermal couples and radiometers.

3 RESULTS AND DISCUSSIONS

3.1 Jet condition

To describe the real-gas behaviour of cryogenic hydrogen, the ideal gas equation of state, Abel-Nobel equation of state (AN-EOS) and the equation of state proposed by Chen *et al*. [30] are compared to the data provided by real properties database of National Institute of Standards and Technology (NIST) [31]. The densities at temperature 100 K and 273 K with pressures ranging from 0~10 bar_{abs} are plotted in Figure 4. While the temperature is equal to 273 K, it is found that the maximum absolute error for the density is 0.00548 kg/m^3 and the maximum relative error is 0.63% when using ideal gas equation of state. However, when the hydrogen temperature drops to 100 K, the deviation of density calculated by ideal gas equation of state reduces to 0.16%, which is the smallest in the three equations of state. The discrepancies predicted by AN-EOS and the equation of state proposed Chen *et al*. are 1.97% and 2.03%, respectively. In this study, the ideal gas equation of state is adopted to describe the behaviour of cryogenic hydrogen.

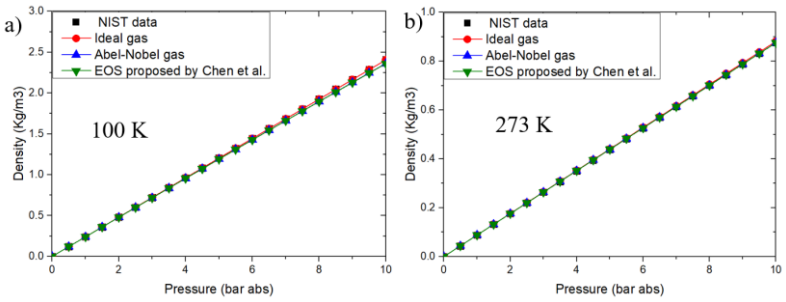

Figure 4. Comparison of real-gas state equations, (a) T=100 K; (b) T=273 K.

The isentropic flow is assumed for cryogenic hydrogen discharge and the parameters at the jet exit can be expressed as [6], [7]

$$P_j = P_o \left(\frac{2}{\gamma+1}\right)^{\gamma/(\gamma-1)} \tag{1}$$

$$T_j = T_0 \cdot \frac{2}{\gamma+1} \tag{2}$$

$$\rho_j = P_o \left(\frac{2}{\gamma+1}\right)^{1/(\gamma-1)} \frac{M}{RT_0} \tag{3}$$

$$U_j = \sqrt{\frac{RT_0}{M}\left(\frac{2\gamma}{\gamma+1}\right)} \tag{4}$$

where the subscripts 0 and j refer to the conditions in the stagnation chamber and at the jet exit, respectively.

3.2 Flame length

Delichatsios [9], [32] defined a dimensionless flame length L^* based on the flame Froude number that measures the ratio of buoyancy-to-momentum forces in jet flame. The flame Froude number is defined as:

$$Fr_f = \frac{U_j {f_s}^{3/2}}{(\rho_j/\rho_\infty)^{1/4}[(\Delta T_f/T_\infty) g d_j]^{1/2}} \tag{5}$$

where U_j is the velocity at jet nozzle, f_s is the mass fraction of fuel at stoichiometric conditions, ρ_j/ρ_∞ is the ratio of jet gas density to ambient gas density, ΔT_f is the peak flame temperature rise due to combustion, T_∞ is the ambient temperature and d_j is jet nozzle diameter. The dimensionless flame length can be expressed as

$$L^* = \frac{L_f f_s}{d^*} = \frac{L_f f_s}{d_j(\rho_j/\rho_\infty)^{1/2}} \tag{6}$$

where L_f is the visible flame length. Schefer *et al*. [9] used a piecewise function to correlate the flame length with the flame Froude number. For a buoyancy-dominated flame with $Fr_f < 5$, L^* is correlated by the expression

$$L^* = \frac{13.5 {Fr_f}^{2/5}}{(1+0.07 {Fr_f}^2)^{1/5}} \tag{7}$$

and $L^* = 23$ for the momentum-dominated hydrogen jet with $Fr_f > 5$.

In Figure 5, the dimensionless flame lengths of cryogenic hydrogen jet fires measured in this study are compared to the flame lengths reported by different authors [9], [11], [26], [33], [34]. For the buoyancy-dominated flames, the correlation is in good agreement with experimental data. However, around the line $L^* = 23$, there is a large scatter of both the cryogenic hydrogen jet fire data and those at the room temperature, which have also been reported by Molkov *et al*. [35]. It is found that the correlation based on the flame Froude number cannot be applied to high-momentum or cryogenic hydrogen jet fire successfully.

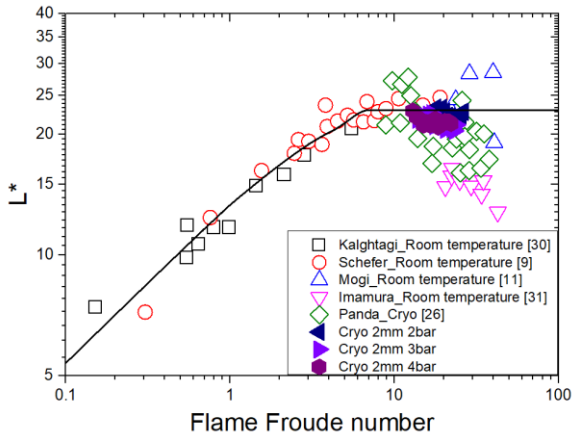

Figure 5. Correlation between the dimensionless flame length, L* and the flame Froude number for the cryogenic hydrogen jet fires in this work, along with data from literature [9], [11], [26], [33], [34].

Panda *et al.* [26] carried out a series of cryogenic hydrogen fire experiments and developed a correlation to express the normalized flame length, L_f/d_j, as a function or the Reynolds number at the jet nozzle. The normalized flame length is defined by the expression

$$L_f/d_j = 0.86\sqrt{Re} \tag{8}$$

Figure 6 shows the variation of normalized flame lengths as a function of the square root of Reynolds number in the current study, along with the data from literature [9], [11], [26], [36]. The black solid line in Figure 5 represents Equation (4). The data of cryogenic hydrogen flame lengths in current study and from Panda *et al*. [26] are in good agreement with Equation (4), however, the experimental data at room temperature are seriously scattered.

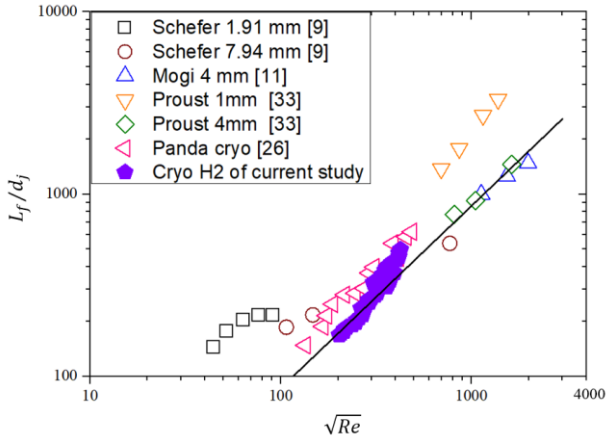

Figure 6. Correlation between the dimensionless flame length, L_f/d_j and the Reynolds number for the cryogenic hydrogen jet fires in this work, along with data from literature [9], [11], [26], [36].

Mogi *et al*. [11] measured the visible flame length L_f and flame width W_f for hydrogen jet fire with pressures ranging from 0.1 to 45 MPa at room temperature and developed a dependence on the stagnation pressure p_0 and jet nozzle diameter d_j. The equations can be expressed as:

$$L_f/d_j = 530{p_0}^{0.43} \tag{9}$$

$$W_f/d_j = 95{p_0}^{0.43} \tag{10}$$

However, these equations do not demonstrate the dependence of the flame length or width on the release temperature of hydrogen jets, which may cause a large deviation from the values at room temperature [27]. Figure 7 presents the variation of the shape and lengths of hydrogen jet fire with temperature under the condition of 3 mm jet nozzle and 4 bar_{abs}. The flame length increases by 32.6% from 0.92 to 1.22 m while the temperature decreases by 100 K from 273 K to 173 K. To unify the correlations at room and low temperature, we express the normalized flame length, L_f/d_j, as a function of stagnation pressure, p_0 and the temperature ratio, T_{atm}/T_{stag}. The coefficients in Equations (5) and (6) are not changed to ensure the availability at room temperature. Figure 8 shows the variation of normalized flame length of the cryogenic hydrogen jet fires in the current study, along with the data from literature [11], [26], [27]. The data follows a line with the equation of the best fit given by

$$L_f/d_j = 530{p_0}^{0.43}\left(\frac{T_{atm}}{T_{stag}}\right)^{0.35} \tag{11}$$

where T_{atm} and T_{stag} are the ambient temperature and the temperature in the stagnation chamber. Besides, the relation between the flame length L_f and the maximum flame width W_f is plotted in Figure 9. The flame width correlates to the flame length and is approximately equal to $0.18L_f$. Similar to the correlation proposed by Mogi *et al.* [11], we can obtain the following equation from Equation (5):

$$W_f/d_j = 95{p_0}^{0.43}\left(\frac{T_{atm}}{T_{stag}}\right)^{0.35} \tag{12}$$

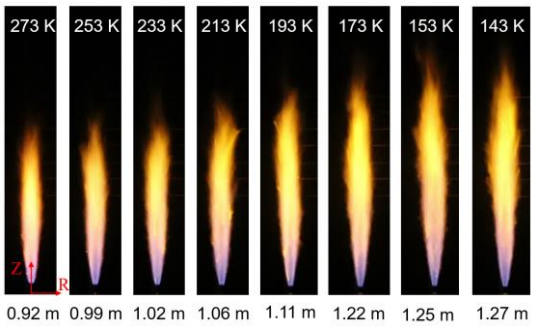

Figure 7. Variation of flame shape and lengths at variable stagnation temperature for the scenario of 3 mm jet nozzle and 4 bar.

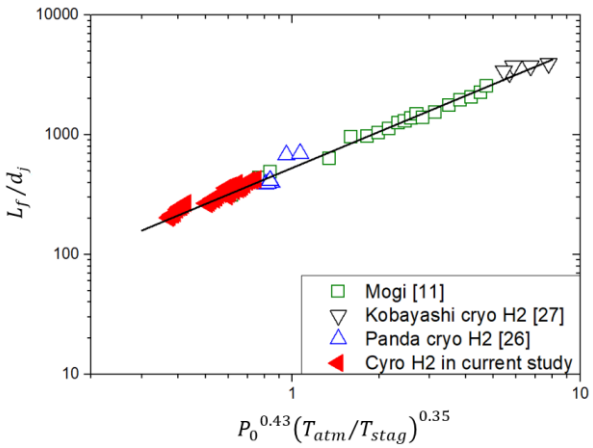

Figure 8. Variation of the dimensionless flame length, L_f/d_j, as a function of stagnation pressure and temperature ratio, T_{atm}/T_{stag} in this work, along with data from literature [11], [26], [27].

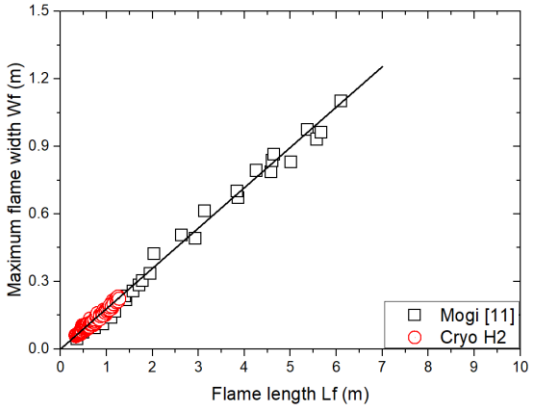

Figure 9. Relations between the maximum flame width and the flame length in this work, along with data from literature.

3.3 Radiant heat flux

Radiant heat flux of hydrogen jet fires is a key parameters for the development of hydrogen safety codes and standards. To characterize the thermo-physical properties of cryogenic-compressed hydrogen jet fire in this study, the radiant heat flux was measured along the flame length by four Captec radiometers. Figure 10 shows the axial variation of the radiative heat flux measured by the radiometers for five scenarios at different stagnation temperatures. The axial locations of the radiometers on Z axis are normalized by the measured flame lengths, respectively, and the peak values of radiative heat flux are observed at Z/L_f in the range of 0.65-0.85. It is also noticeable that, with the decrease of stagnation temperature, the normalized height Z/L_f of peak position decreases under the same pressure.

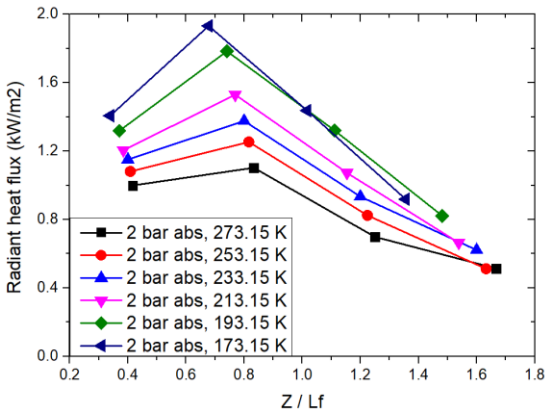

Figure 10. Radiative heat fluxes along the hydrogen jet axis (jet nozzle diameter is 2 mm and the pressure is 2 bar_{abs}).

Figure 11 shows the variation of radiant heat flux measured by each radiometer as a function of the normalized position Z/L_f. It can be seen that all the measured radiant heat fluxes are negatively correlated with the normalized position Z/L_f of the radiometers. According to the previous section, the flame length increases with the decrease of hydrogen temperature, and the normalized position Z/L_f of each radiometer decreases correspondingly. It is found that the decrease of hydrogen temperature could enhance the thermal radiation from the jet fire.

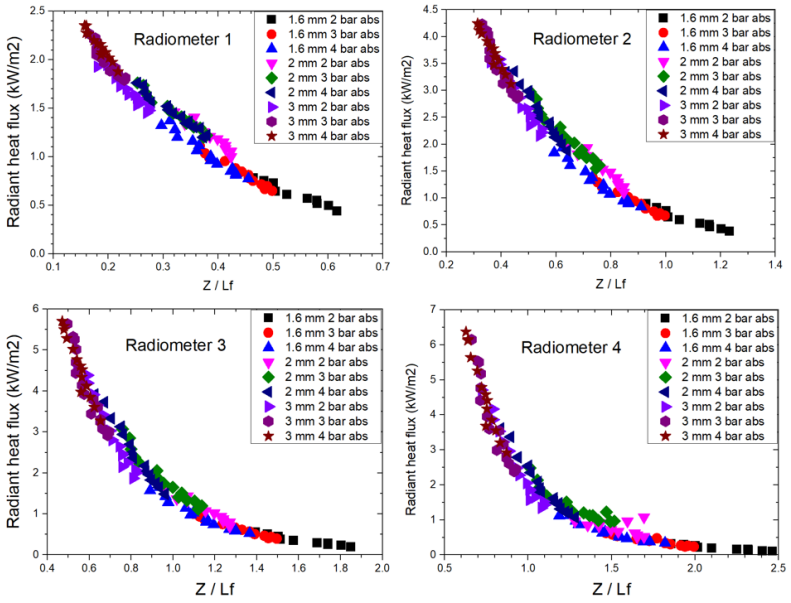

Figure 11. Variation of radiative heat flux as a function of normalized position Z/L_f of each radiometer for all scenarios.

The radiation fraction χ_{rad} is a significant parameter to characterize the radiative properties of vertical hydrogen jet fire. The radiation fraction for turbulent jet flame can be scaled as a function of [37]

$$\chi_{rad} = \frac{S_{rad}}{m_{fuel}\Delta H_c} \propto \tau_f a_p T_{ad}^4 \tag{13}$$

where S_{rad} is the total radiative power emitted from the flame, ΔH_c is the release power due to combustion, m_{fuel} is the mass flow, a_p is the Planck-mean absorption coefficient (0.23 for hydrogen) which can be obtained based on the RADCAL calculations reported by Molina *et al*. [12], T_{ad} is the adiabatic flame temperature and τ_f is the global flame residence time which is defined as

$$\tau_f = \frac{\rho_f {W_f}^2 L_f f_s}{3\rho_j {d_j}^2 U_j} \tag{14}$$

where ρ_f, W_f and L_f are the flame density, width and length, f_s is the mass fraction of fuel at stoichiometric conditions, ρ_j and U_j are the density and velocity at jet nozzle, d_j is the diameter of hydrogen jet nozzle. For turbulent jet flame, the radiative power S_{rad} can be expressed in terms of a dimensionless radiant power, C^*, as below

$$C^*\left(\frac{x}{L}\right) = \frac{4\pi R^2 q_r\left(\frac{x}{L_f}\right)}{S_{rad}} = \frac{4\pi R^2 q_r\left(\frac{x}{L_f}\right)}{\chi_{rad} m_{fuel}\Delta H_c} \tag{15}$$

where x and R are the axial and radial distance between the radiometer and the jet exit. This equation was verified by Sivathanu *et al*. [38] over a range of conditions.

Figure 12 presents the variation of radiation fraction of jet fire as a function of hydrogen temperature. It can be found that the radiation fraction increases with the decrease of hydrogen temperature. As shown in Equation (4), the velocity at the jet exit decreases as the temperature decreases. Besides, according to the analysis in the previous section, the flame length and width increase with the decrease of temperature. Correspondingly, when hydrogen temperature decreases, the global residence time and the radiant fraction increase according to Equation (13) and (14). The increased total radiative power

and radiation fraction from these cryogenic releases must be accounted for in the analysis of the safety associated with cryogenic hydrogen infrastructure.

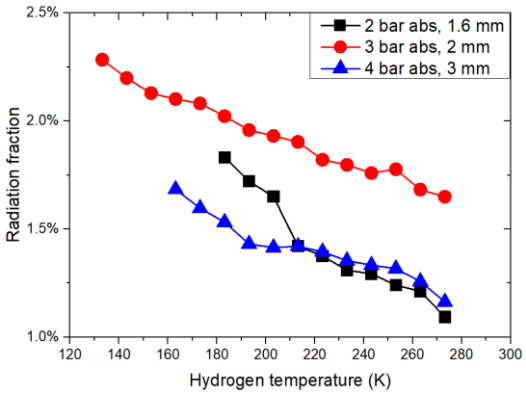

Figure 12. Variation of radiation fraction as a function of hydrogen temperature.

In Figure 13, the calculated radiation fractions are plotted as a function of ${\tau_f a_p T_{ad}}^4$, along with data from literature [12], [26], [39]. Molina *et al*. [12] proposed a correlation as below

$$\chi_{rad} = 0.085 \log_{10}\left({\tau_f a_p T_{ad}}^4\right) - 1.16 \tag{16}$$

which is shown by the yellow dash line in the plot. It can be seen that the when the value of ${\tau_f a_p T_{ad}}^4$ is between 1E13 and 1E14 $ms \cdot m^{-1} \cdot K^4$, there is a large scatter of the current data and the cryogenic data obtained by Panda *et al*. [26]. A correlation based on piecewise polynomial law is proposed to predict the radiative fraction as a function of global flame residence time, given as

$$\chi_{rad} = \begin{cases} 0.013 \log_{10}\left({\tau_f a_p T_{ad}}^4\right) - 1.56 \; if \; {\tau_f a_p T_{ad}}^4 < 1.5 \times 10^{14} \; ms \cdot m^{-1} \cdot K^4 \\ 0.107 \log_{10}\left({\tau_f a_p T_{ad}}^4\right) - 1.49 \; if \; {\tau_f a_p T_{ad}}^4 > 1.5 \times 10^{14} \; ms \cdot m^{-1} \cdot K^4 \end{cases} \tag{17}$$

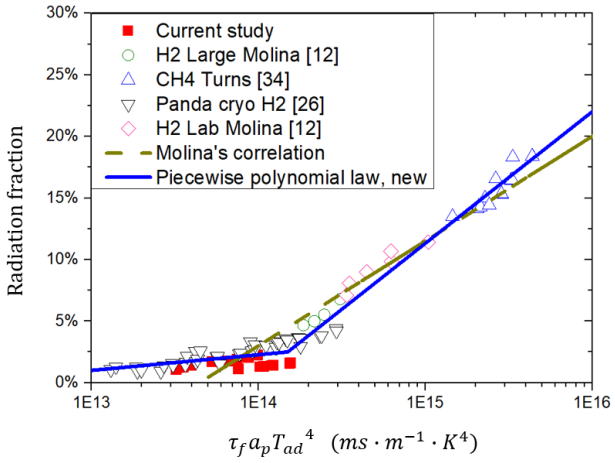

Figure 13. Calculated radiation fractions for the cryogenic hydrogen jet fires in this work, along with data from literature.

REFERENCES

[1] T. Brown, L. S. Schell, S. Stephens-Romero, and S. Samuelsen, "Economic analysis of near-term California hydrogen infrastructure," *Int. J. Hydrogen Energy*, vol. 38, no. 10, pp. 3846–3857, 2013.

[2] N. 2. Q. M. National fire protection agency, *Hydrogen Technologies Code*. 2016.

[3] et al. Ekoto IW, Hecht E, San Marchi C, Groth KM, Lafleur AC, Natesan N, “Liquid hydrogen release and behavior modeling: state-of-the-art knowledge gaps and research needs for refueling infrastructure safety.”

[4] A. J. Ruggles and I. W. Ekoto, “Ignitability and mixing of underexpanded hydrogen jets,” *Int. J. Hydrogen Energy*, vol. 37, no. 22, pp. 17549–17560, 2012.

[5] X. Li *et al.*, “Measurements of concentration decays in underexpanded jets through rectangular slot nozzles,” *Int. J. Hydrogen Energy*, vol. 43, no. 20, pp. 9884–9893, 2018.

[6] A. D. Birch, D. R. Brown, M. G. Dodson, and F. Swaffield, “The Structure and Concentration Decay of High Pressure Jets of Natural Gas,” *Combust. Sci. Technol.*, vol. 36, no. 5–6, pp. 249–261, 1984.

[7] A. D. Birch, D. J. Hughes, and F. Swaffield, “Velocity Decay of High Pressure Jets,” *Combust. Sci. Technol.*, vol. 52, no. 1–3, pp. 161–171, 1987.

[8] B. C. R. Ewan and K. Moodie, “Structure and Velocity Measurements in Underexpanded Jets,” *Combust. Sci. Technol.*, vol. 45, no. 5–6, pp. 275–288, 1986.

[9] R. W. Schefer, W. G. Houf, T. C. Williams, B. Bourne, and J. Colton, “Characterization of high-pressure, underexpanded hydrogen-jet flames,” *Int. J. Hydrogen Energy*, vol. 32, no. 12, pp. 2081–2093, 2007.

[10] C. Proust, D. Jamois, and E. Studer, “High pressure hydrogen fires,” *Int. J. Hydrogen Energy*, vol. 36, no. 3, pp. 2367–2373, 2011.

[11] T. Mogi and S. Horiguchi, “Experimental study on the hazards of high-pressure hydrogen jet diffusion flames,” *J. Loss Prev. Process Ind.*, vol. 22, no. 1, pp. 45–51, 2009.

[12] A. Molina, R. W. Schefer, and W. G. Houf, “Radiative fraction and optical thickness in large-scale hydrogen-jet fires,” *Proc. Combust. Inst.*, vol. 31, no. 2, pp. 2565–2572, 2007.

[13] K. Matsuura, H. Kanayama, H. Tsukikawa, and M. Inoue, “Numerical simulation of leaking hydrogen dispersion behavior in a partially open space,” *Int. J. Hydrogen Energy*, vol. 33, no. 1, pp. 240–247, 2008.

[14] J. Zhang, M. A. Delichatsios, and A. G. Venetsanos, “Numerical studies of dispersion and flammable volume of hydrogen in enclosures,” *Int. J. Hydrogen Energy*, vol. 35, no. 12, pp. 6431–6437, 2010.

[15] X. Tang, M. Asahara, A. K. Hayashi, and N. Tsuboi, “Numerical investigation of a high pressure hydrogen jet of 82 MPa with adaptive mesh refinement: The starting transient evolution and Mach disk stabilization,” *Int. J. Hydrogen Energy*, vol. 42, no. 10, pp. 7120–7134, 2017.

[16] X. Tang, E. Dzieminska, M. Asahara, A. K. Hayashi, and N. Tsuboi, “Numerical investigation of a high pressure hydrogen jet of 82 MPa with adaptive mesh refinement: Concentration and velocity distributions,” *Int. J. Hydrogen Energy*, vol. 43, no. 18, pp. 9094–9109, 2018.

[17] J. yuan Qian, X. juan Li, Z. xin Gao, and Z. jiang Jin, “A numerical study of unintended hydrogen release in a hydrogen refueling station,” *Int. J. Hydrogen Energy*, vol. 45, no. 38, pp. 20142–20152, 2020.

[18] H. Hussein, S. Brennan, and V. Molkov, “Dispersion of hydrogen release in a naturally ventilated covered car park,” *Int. J. Hydrogen Energy*, vol. 45, no. 43, pp. 23882–23897, 2020.

[19] J. yuan Qian, X. juan Li, Z. xin Gao, and Z. jiang Jin, “A numerical study of hydrogen leakage and diffusion in a hydrogen refueling station,” *Int. J. Hydrogen Energy*, vol. 45, no. 28, pp. 14428–14439, 2020.

[20] W. Houf and R. Schefer, “Predicting radiative heat fluxes and flammability envelopes from unintended releases of hydrogen,” *Int. J. Hydrogen Energy*, vol. 32, no. 1, pp. 136–151, 2007.

[21] P. S. Ã. Cumber, “Efficient calculation of the radiation heat flux surrounding a jet fire,” vol. m, pp. 580–589, 2009.

[22] S. L. Brennan, D. V Makarov, and V. Molkov, “LES of high pressure hydrogen jet fire,” *J. Loss Prev. Process Ind.*, vol. 22, no. 3, pp. 353–359, 2009.

[23] D. M. C. Cirrone, D. Makarov, and V. Molkov, “Simulation of thermal hazards from hydrogen under-expanded jet fire,” *Int. J. Hydrogen Energy*, vol. 44, no. 17, pp. 8886–8892, 2019.

[24] S. G. Giannissi, A. G. Venetsanos, N. Markatos, and J. G. Bartzis, “CFD modeling of hydrogen dispersion under cryogenic release conditions,” *Int. J. Hydrogen Energy*, vol. 39, no. 28, pp. 15851–15863, 2014.

[25] A. Friedrich *et al.*, “Ignition and heat radiation of cryogenic hydrogen jets,” *Int. J. Hydrogen Energy*, vol. 37, no. 22, pp. 17589–17598, 2012.

[26] P. P. Panda and E. S. Hecht, “Ignition and flame characteristics of cryogenic hydrogen releases,” *Int. J. Hydrogen Energy*, vol. 42, no. 1, pp. 775–785, 2017.

[27] H. Kobayashi *et al.*, “Experimental study on cryo-compressed hydrogen ignition and flame,” *Int. J. Hydrogen Energy*, vol. 45, no. 7, pp. 5098–5109, 2020.

[28] E. Studer, D. Jamois, S. Jallais, G. Leroy, J. Hebrard, and V. Blanchetière, “Properties of large-scale methane/hydrogen jet fires,” *Int. J. Hydrogen Energy*, vol. 34, no. 23, pp. 9611–9619, 2009.

[29] J. LaChance, “Risk-informed separation distances for hydrogen refueling stations,” *Int. J. Hydrogen Energy*, vol. 34, no. 14, pp. 5838–5845, 2009.

[30] H. Chen, J. Zheng, P. Xu, L. Li, Y. Liu, and H. Bie, “Study on real-gas equations of high pressure hydrogen,” *Int. J. Hydrogen Energy*, vol. 35, no. 7, pp. 3100–3104, 2010.

[31] P. J. Linstrom and W. G. Mallard, “The NIST Chemistry WebBook : A chemical data resource on the internet,” *J. Chem. Eng. Data*, vol. 46, no. 5, 2001.

[32] M. A. Delichatsios, “Transition from momentum to buoyancy-controlled turbulent jet diffusion flames and flame height relationships.”

[33] T. Gautam, “Lift-off Heights and Visible Lengths of Vertical Turbulent Jet Diffusion Flames in Still Air,” *Combust. Sci. Technol.*, vol. 41, no. 1–2, pp. 17–29, 2010.

[34] T. Imamura *et al.*, “Experimental investigation on the thermal properties of hydrogen jet flame and hot currents in the downstream region,” *Int. J. Hydrogen Energy*, vol. 33, no. 13, pp. 3426–3435, 2008.

[35] V. Molkov and J. B. Saffers, “Hydrogen jet flames,” *Int. J. Hydrogen Energy*, vol. 38, no. 19, pp. 8141–8158, 2013.

[36] C. Proust, D. Jamois, and E. Studer, “High pressure hydrogen fires,” *Int. J. Hydrogen Energy*, 2011.

[37] S. R. Turns and F. H. Myhr, “Oxides of nitrogen emissions from turbulent jet flames: Part I—Fuel effects and flame radiation,” *Combust. Flame*, vol. 87, no. 3, pp. 319–335, 1991.

[38] Y. R. Sivathanu and J. P. Gore, “Total radiative heat loss in jet flames from single point radiative flux measurements,” *Combust. Flame*, vol. 94, no. 3, pp. 265–270, 1993.

[39] S. R. Turns, F. H. Myhr, R. V. Bandaru, and E. R. Maund, “Oxides of nitrogen emissions from turbulent jet flames: Part II-Fuel dilution and partial premixing effects,” *Combust. Flame*, vol. 93, no. 3, pp. 255–269, 1993.